NASA Contractor Report 4608

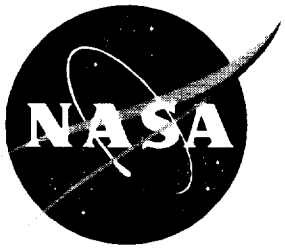

Strength Evaluation of Socket Joints

Larry C. Rash
Calspan Corporation • Tullahoma, Tennessee

National Aeronautics and Space Administration
Langley Research Center • Hampton, Virginia 23681-0001

Prepared for Langley Research Center
under Contract NAS1-19385

June 1994

STRENGTH EVALUATION OF SOCKET JOINTS

Table of Contents

INTRODUCTION

The results included in this report were previously released as a company report, see Reference 1, and this report is intended to formalize that analysis and to document the results of a validation study that was performed later and included here as Appendix B. Prior to that analysis, the stresses in the joints of the model support systems were resolved by assuming the moment in the joint was reacted about the center of the joint and the stresses were the result of this moment that were reacted over a plane parallel to the horizontal centerline. The new analytical technique was developed to better define the loads and stresses in typical sting joints found in the model support systems at the National Transonic Facility at NASA LaRC and to provide a design tool that could easily be used during the design of new model support systems. To be more precise, the original objective was to provide a method of determining the loads and stresses in concentric, tapered, socket type joints found in wind tunnel model support systems. Once completed, the analytical method was found to be applicable to any overlapping type joint. Some joints for which the method is applicable are illustrated in Figure 1 and includes general configurations where one of the joint members can be considered to be basically supported by the contact pressure from the other joint member. The forward end of a model support system engages with and is supported by an aft support system, which is the subject of this report. A lamppost is supported by the ground and the analytical technique included herein can be used to determine if the depth of penetration is sufficient for the bearing pressure of the soil to laterally support the lamppost during high wind conditions. The strength of a clamped round bar assembly and the strength of a tongue and groove type joint that are subjected to external forces and moments can both be evaluated using this analytical technique. The tongue and groove joint would, however, require some additional development to determine the proper stress relationships which could be accomplished by a similar analysis to what is included here by using strip theory to evaluate the strength of a unit width of the joint.

The results in this report are in the form of equations that are for a concentric, tapered socket type joint and can be used during the design of new model support systems to determine the strength of socket joints and for most applications the need of more lengthy analyses can be avoided. Results are provided for both a joint where the joint members are in continuous contact along the full length of the joint and for a joint with intermediate contact relief. The joint with intermediate contact relief has a gap between the joint members along about one-third of the midsection of the joint, typical of

NASA LaRC sting joints, and the joint members are in full contact fore and aft of this midsection gap. Illustrations of both joint types are given in Figures 2 and 3. Analytically, the approach for both was to use Strength of Materials principles to analyze the joint members by idealizing the joint as two rigid, parallel beams that are joined by an infinite number of springs along the contacting surfaces. The contact loads can be pictured as being equivalent to the loads developed in the springs along the length of the joint attributed to the differential slope between two rigid joint members. The contact loads between the joint members are represented as externally applied, linearly varying, distributed loads and are as shown on the free body diagrams in Figure 2 and 3. Each joint member is treated like a simple beam and the contact loads between the beams are taken to act like external loads that are independently applied to each of the two beams. For the first joint member, depicted in Figures 2b and 3b, the externally applied loads are balanced by the application of the contact type loads and for the second joint member, depicted in Figures 2c and 3c, the contact loads are the only loads that act on the end of the cantilevered beams. These contact loads, in conjunction with the externally applied loads for the forward joint members are used to develop independent expressions for the bending moment along the length of the joint for the two joint members. The joint stress relationships for the joint members are determined from the bending moment equations by including the effects of appropriate section properties for a given geometry. The geometry of the contacting surfaces for the joint in this report is in the shape of a frustum of a cone and is representative of the tapered socket type joints found in model support systems in NASA LaRC wind tunnels.

The results in this report can be used to determine the distributed contact loads and stresses in sting joints directly from joint dimensions and externally applied loads. As a design aid, the key equations have been programed for a personal computer to automatically compute all the results given in this report. A copy of an IBM BASIC program that was developed to evaluate the results for a concentric tapered, socket type joint is included as Appendix A.

ANALYSIS

FORWARD JOINT MEMBER WITH CONTINUOUS CONTACT

Load Development

To identify the stresses in the joint, the contact loads can be used to evaluate distributed bending moments and ultimately the stresses. Expressions for distributed loads can be developed in terms of the externally applied loads by assuming a linear load variation along the longitudinal axis of the beam members attributed to the contact pressure and solving for maximum magnitudes of the distributed loads required to achieve equilibrium. The direction of the loading reverses at some intermediate location which is literally where the contact loads shift from the upper mating surface to the lower mating surface and this load reversal location can be used as a dependent variable to simplify other expressions. To solve for this load reversal location, consider that there are two other unknowns which are the maximum magnitudes of the distributed loads at each end of the joint, or the concentrated loads that are equivalent to the distributed loads, and three equations will therefore be required for a unique solution. Summation of forces and moments provide two of the equations and an assumption that the distributed loads are linear provides the basis for a third equation. For an illustration of the loads and relevant dimensions refer to Figure 2b. Summing forces in the vertical direction for the forward joint member yields

$$F_0 - W_1 + W_2 = 0 \tag{1}$$

Summing moments about the load center of the externally applied loads, F_0 and M_0, provides

$$M_0 + W_1\left[L - b + \frac{(b-a-c)}{3} \right] - W_2\left[L - a - \frac{c}{3} \right] = 0 \tag{2}$$

For the linear variation assumption, the loads can be related by using the geometric properties of similar triangles (the ratio of all corresponding sides of similar triangles are equal)

$$\frac{w_1}{(b-a-c)} = \frac{w_2}{c} \tag{3}$$

To equate the preceding equations, expressions for the distributed loads given in equation (3) can be determined in terms of concentrated loads, using a basic definition that an equivalent concentrated load for a linearly varying distributed load that goes to zero is half the product of the peak distributed load times the distance over which the load acts. The following relationships are rearranged to solve for the distributed loads in terms of the concentrated loads.

$$w_1 = \frac{2W_1}{b - a - c} \tag{4}$$

$$w_2 = \frac{2W_2}{c} \tag{5}$$

substituting equations (4) and (5) into equation (3) gives the following relationship between the equivalent concentrated loads after grouping

$$\left[(b-a)^2 - 2c(b-a) + c^2\right] W_2 - c^2 W_1 = 0 \tag{3a}$$

Three linearly independent equations, (1), (2), and (3a) are now available that can be solved simultaneously for the three unknowns (c, W_1 and W_2) in terms of the externally applied loads (F_0 and M_0) and the joint dimensions as shown in Figure 2. The load reversal location would be

$$c = \frac{3(b-a)\left[M_0 + F_0(L-a)\right] - 2(b-a)^2 F_0}{6\left[M_0 + F_0(L-a)\right] - 3(b-a)F_0} \tag{6}$$

To simplify the following expressions for the equivalent concentrated loads, the equations are expressed in terms of the load reversal location, c, which is defined in the preceeding equation

$$W_1 = \frac{3\left[M_0 + F_0(L-a)\right] - cF_0}{2(b-a)} \tag{7}$$

$$W_2 = \frac{3\left[M_0 + F_0(L-a)\right] - \left[c + 2(b-a)\right] F_0}{2(b-a)} \tag{8}$$

The dimension identifying the load reversal location, c, can also be used to simplify the expression for the varying contact load and will be used in the following development as an independent variable. The dimension identifies the physical location where the contact loads shift from the upper mating surfaces to the lower mating surfaces and distinguishes where separate governing equations are required for the downward acting loads and for the upward acting loads, see Figure 2.

Forward Bending Moment Equation

Expressions for the bending moment at any location along the length of the joint can be developed in terms of the downward acting contact loads by considering the forward load segment as a function of the x-distance along the beam, see adjacent figure. Again, using similar triangles, the magnitude of this partial distributed load at some general distance "x" from the external loads would be

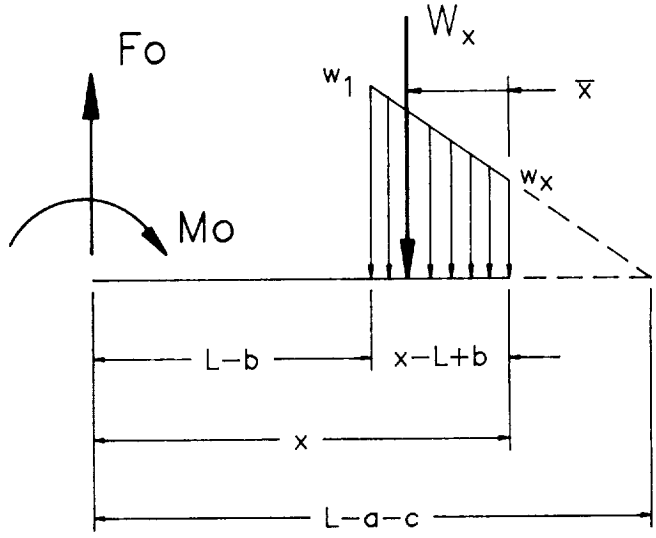

$$w_x = \left(\frac{L\text{-}a\text{-}c\text{-}x}{b\text{-}a\text{-}c}\right) w_1 \quad \text{for } L - b \leq x \leq L - a - c \tag{9}$$

The variable concentrated load in terms of the partial distributed load up to the point of evaluation would be

$$W_x = \frac{w_1}{2}\left[\frac{L\text{-}x\text{+}b\text{-}2(a\text{+}c)}{b\text{-}a\text{-}c}\right](x\text{-}L\text{+}b) \quad \text{for } L - b \leq x \leq L - a - c \tag{10}$$

expressing in terms of the total concentrated load, W_1, using equation (4)

$$W_x = W_1\left\{\frac{[L\text{-}x\text{+}b\text{-}2(a\text{+}c)]}{(b\text{-}a\text{-}c)^2}\right\}(x\text{-}L\text{+}b) \quad \text{for } L - b \leq x \leq L - a - c \tag{11}$$

The distance from the center of this variable concentrated load to the section at which the bending moment is being evaluated, see above figure, can be evaluated as if it was a homogeneous plane section by using the distributed loads as equivalent to any other dimension.

$$\bar{x}_x = \frac{w_x(x\text{-}L\text{+}b)\left(\frac{x\text{-}L\text{+}b}{2}\right) + \frac{1}{2}(w_1 - w_x)(x\text{-}L\text{+}b)\frac{2}{3}(x\text{-}L\text{+}b)}{w_x(x\text{-}L\text{+}b) + \frac{1}{2}(w_1 - w_x)(x\text{-}L\text{+}b)} \quad \text{for } L - b \leq x \leq L - a - c$$

Simplifying

$$\bar{x}_x = \frac{(x\text{-}L\text{+}b)(w_x + 2w_1)}{3(w_x + w_1)} \quad \text{for } L - b \leq x \leq L - a - c \tag{12}$$

substituting for w_x, using equations (9), and simplifying yields the following expression for the distance to the load center location.

$$\bar{x}_x = \frac{(x\text{-}L\text{+}b)}{3}\left[\frac{3(b\text{-}a\text{-}c) - (x\text{-}L\text{+}b)}{L\text{-}x\text{+}b\text{-}2(a\text{+}c)}\right] \quad \text{for } L - b \leq x \leq L - a - c \tag{13}$$

The expression for the general bending moment at any location along the forward end of the joint would be the product of the variable concentrated load, W_x, and the distance to its respective load center, $\bar{x}_x$, in combination with the moment attributed to the externally applied loads M_0 and F_0

$$M_x = M_0 + F_0x - W_x\bar{x}_x \qquad \text{for } L\text{-}b \leq x \leq L\text{-}a\text{-}c$$

Substituting for W_x and $\bar{x}_x$, using equations (11) and (13), and simplifying provides the final expression of the bending moment for the forward end of the joint (note that a similar expression can be found in Reference 3 for a cantilever with a partial triangular load)

$$\boxed{M_x = M_0 + F_0x - \frac{W_1}{3}\left[\frac{3(x\text{-}L\text{+}b)^2}{(b\text{-}a\text{-}c)} - \frac{(x\text{-}L\text{+}b)^3}{(b\text{-}a\text{-}c)^2}\right] \text{ for } L\text{-}b \leq x \leq L\text{-}a\text{-}c} \tag{14}$$

where c and W_1 are determined from equations (6) and (7).

Aft Bending Moment Equation

For the aft end of the joint, a similar expression is required which is a function of the preceding terms and also the upward acting distributed load that starts at the load reversal location, see adjacent figure. The general bending moment aft of the load reversal location in terms of a newly defined variable concentrated load, W_x, and the distance to its load center, $\bar{x}_x$, can then be expressed as follows:

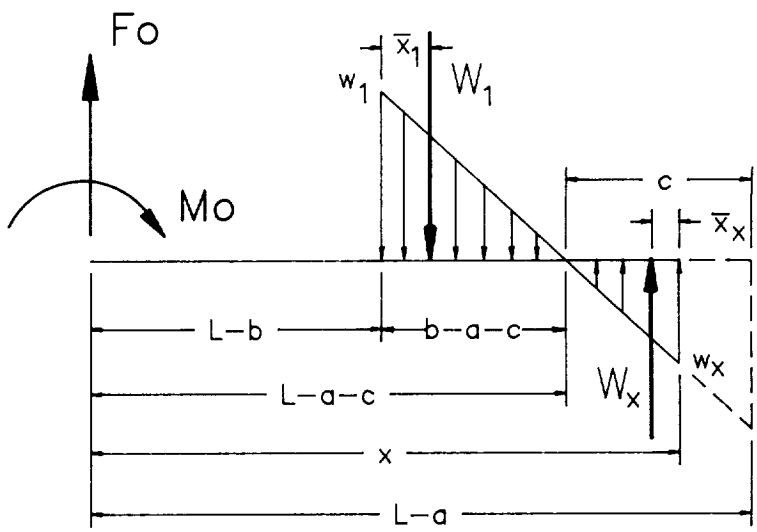

$$M_x = M_0 + F_0x - W_1\left[x - (L - b) - \left(\frac{b - a - c}{3}\right)\right] + W_x\bar{x}_x \quad \text{for } L\text{-}a\text{-}c \leq x \leq L\text{-}a \qquad (15)$$

where $\frac{(b - a - c)}{3}$ is $\bar{x}_1$.

To determine a new expression for the variable concentrated load at the aft end of the joint start with a general expression of the partial distributed load at the location of the evaluation in terms of the aft distributed load

$$w_x = \left(\frac{x\text{-}L+a+c}{c}\right)w_2 \quad \text{for } L\text{-}a\text{-}c \leq x \leq L\text{-}a \qquad (16)$$

which in terms of the equivalent concentrated load from equation (5) would be

$$w_x = \frac{2(x\text{-}L+a+c)}{c^2}W_2 \quad \text{for } L\text{-}a\text{-}c \leq x \leq L\text{-}a \qquad (17)$$

The general expression for the variable concentrated load at the aft end of the joint can then be expressed in terms of the distributed load as

$$W_x = \tfrac{1}{2}w_x(x\text{-}L+a+c) \quad \text{for } L\text{-}a\text{-}c \leq x \leq L\text{-}a \qquad (18)$$

and in terms of the total concentrated aft load would be

$$W_x = W_2\left(\frac{x\text{-}L+a+c}{c}\right)^2 \quad \text{for } L\text{-}a\text{-}c \leq x \leq L\text{-}a \tag{19}$$

The distance from the location of the evaluation to this aft centroid would be

$$\bar{x}_x = \frac{1}{3}(x\text{-}L+a+c) \quad \text{for } L\text{-}a\text{-}c \leq x \leq L\text{-}a \tag{20}$$

The final expression of the general bending moment at any location along the aft end of the joint, after substituting equation (19) for the concentrated load into equation (15) and equation (20) for the centrodial distance, can be expressed as

$$M_x = M_0 + F_0 x - W_1\left[(x\text{-}L+b) - \left(\frac{b\text{-}a\text{-}c}{3}\right)\right] + W_2\frac{(x\text{-}L+a+c)^3}{3c^2}$$

$$\text{for } L\text{-}a\text{-}c \leq x \leq L\text{-}a \tag{21}$$

where c, W_1 and W_2 are determined from equations (6), (7) and (8).

Note that at x = L - a - c either equation (14) or equation (21) can be used to evaluate the bending moment since they are algebraically identical.

BENDING MOMENT EQUATIONS FOR AFT JOINT MEMBER WITH CONTINUOUS CONTACT

For the aft joint member, the loading is purely through the contact loads and the external loads, M_0 and F_0, would not appear directly in the expressions for the bending moment equations, see Figure 2c. The bending moment equations for the aft joint member would be similar to the equations for the forward joint member with the only differences being the omission of the externally applied loads, M_0 and F_0, and a sign change to indicate that the loads act in the opposite direction. The general expression for the bending moment equations for the aft joint member can therefore be obtained directly from previous equations by simply omitting the external load terms and by changing the sign of the concentrated load terms to reflect loads are in the opposite direction. Revising equation (14) yields the following general bending moment equation for the forward end of the aft joint member

$$M_x = \frac{W_1}{3}\left[\frac{3(x - L + b)^2}{b - a - c} - \frac{(x - L + b)^3}{(b - a - c)^2}\right] \quad \text{for } L - b \leq x \leq L - a - c \tag{22}$$

where c and W_1 are determined from equations (6) and (7).

Revising equation (21) yields the following general bending moment equation for the aft end of the aft joint member

$$M_x = W_1\left[(x - L + b) - \left(\frac{b - a - c}{3}\right)\right] - W_2 \frac{(x - L + a + c)^3}{3c^2} \quad \text{for } L - a - c \leq x \leq L - a \tag{23}$$

where c, W_1 and W_2 are determined from equations (6), (7) and (8).

FORWARD JOINT MEMBER WITH INTERMEDIATE CONTACT RELIEF

Load Development

Expressions for the loading between two beam members that are not in contact along the full length of the joint can be developed similar to the preceding for the joint with continuous contact. The primary difference is that a third set of independent bending moment equations will be required for the intermediate region where the joints are not in contact, see Figure 3 for dimensions and an illustration of the joint. The load reversal location will again be used even though for this case it is a hypothetical dimension based on a projection of the linearized distributed load and would define where the loading would be zero, if the contact were continuous, see Figure 3b. The load reversal location will generally occur along the intermediate relief region and an expression for its location will be developed later. Summing forces in the vertical direction for the forward joint member would provide the same results as given in equation (1) and summing moments about the load center of the externally applied loads, F_0 and M_0, provides

$$M_0 + W_1(L - b + \bar{x}_1) - W_2(L - a - \bar{x}_2) = 0 \tag{24}$$

Solving equations (1) and (24) simultaneously for the concentrated loads, W_1 and W_2, in terms of the externally applied loads, F_0 and M_0, and the load center locations, $\bar{x}_1$ and $\bar{x}_2$, yields

$$W_1 = \frac{M_0 + (L - a - \bar{x}_2) F_0}{(b - a) - \bar{x}_1 - \bar{x}_2} \tag{25}$$

$$W_2 = \frac{M_0 + (L - b + \bar{x}_1) F_0}{(b - a) - \bar{x}_1 - \bar{x}_2} \tag{26}$$

The load center locations, $\bar{x}_1$ and $\bar{x}_2$, can be determined as before by considering the distributed loading as if it were a homogeneous plane section and the location of the concentrated loads can be evaluated as if they were the centroid locations, see Figure 3 for illustration of dimensions. Solving for the load centers in terms of the distributed loads yield

$$\bar{x}_1 = \frac{e\left(w_1 + 2w_1'\right)}{3\left(w_1 + w_1'\right)} \tag{27}$$

$$\bar{x}_2 = \frac{f\left(w_2 + 2w_2'\right)}{3\left(w_2 + w_2'\right)} \tag{28}$$

The intermediate distributed loads terms, w_1' and w_2', can be eliminated from the above expressions by again using the properties of similar triangles to relate them to the maximum magnitudes of the distributed loads. For an assumed linear variation along the length of the joint, the intermediate distributed loads in terms of the maximum magnitudes of distributed loads and related joint dimensions would be

$$w_1' = \left(\frac{b - a - c - e}{b - a - c}\right) w_1 \tag{29}$$

$$w_2' = \left(\frac{c - f}{c}\right) w_2 \tag{30}$$

Substituting equation (29) into (27) into equation (30) into (28), yields the following expressions for the load center locations, after simplifying

$$\bar{x}_1 = \frac{e}{3}\left[\frac{3(b - a - c) - 2e}{2(b - a - c) - e}\right] \tag{31}$$

$$\bar{x}_2 = \frac{f}{3}\left(\frac{3c - 2f}{2c - f}\right) \tag{32}$$

Note that in the final expressions for the load centers, all the distributed load terms have canceled out and the only remaining terms are the joint dimensions. These expressions for the load centers can now be substituted into the expressions for the concentrated loads, equations (25) and (26), to obtain expressions that are only functions of the externally applied loads, F_0 and M_0, and the joint dimensions

$$W_1 = \frac{M_0 + \left[L - a - \frac{f}{3}\left(\frac{3c - 2f}{2c - f}\right)\right] F_0}{(b - a) - \frac{e}{3}\left[\frac{3(b - a - c) - 2e}{2(b - a - c) - e}\right] - \frac{f}{3}\left(\frac{3c - 2f}{2c - f}\right)} \tag{33}$$

$$W_2 = \frac{M_0 + \left\{L - b + \frac{e}{3}\left[\frac{3(b - a - c) - 2e}{2(b - a - c) - e}\right]\right\} F_0}{(b - a) - \frac{e}{3}\left[\frac{3(b - a - c) - 2e}{2(b - a - c) - e}\right] - \frac{f}{3}\left(\frac{3c - 2f}{2c - f}\right)} \tag{34}$$

The only joint dimension included in the above equations that is not yet known is the load reversal location, c, and it can be determined by starting with the assumption of linear variation in the distributed loads that relates the distributed loads to the joint dimensions, again based on properties of similar triangles.

$$\frac{w_1}{b - a - c} = \frac{w_2}{c} \tag{35}$$

Relationships between the distributed loads and the concentrated loads are needed and can be obtained by considering the concentrated loads are equivalent to the product of the average distributed load times the respective lengths, again see Figure 3b for illustration.

$$W_1 = \left(\frac{w_1 + w_1'}{2}\right) e \tag{36}$$

$$W_2 = \left(\frac{w_2 + w_2'}{2}\right) f \tag{37}$$

Substituting the expressions in equations (29) and (30) into the above equations for the intermediate distributed loads, w_1' and w_2', and solving for the distributed loads, w_1 and $_2$, yields

$$w_1 = \frac{2W_1}{e}\left[\frac{b - a - c}{2(b - a - c) - e}\right] \tag{38}$$

$$w_2 = \frac{2W_2}{f}\left(\frac{c}{2c - f}\right) \tag{39}$$

where W_1 and W_2 are determined from equations (33) and (36) and the load reversal location, c, is determined below.

Substituting equations (38) and (39) into equation (35) and reducing yields

$$W_1 f(2c - f) = W_2 e\,[\,2\,(b - a - c) - e\,] \tag{40}$$

Substituting for W_1 and W_2, using equations (33) and (34), simplifying, and solving for the load reversal location in terms of the externally applied loads and joint dimensions as illustrated in Figure 3b yields

$$c = \frac{\left[2e(b-a)+f^2- e^2\right] M_0+\left\{f^2(L-a) - \frac{2}{3}(f^3+e^3)+e^2[(b-a) - (L-b)]+2(b-a)\,(L-b)\,e\right\} F_0}{2(e + f)\,M_0 + \left\{2[f(L-a) + e(L-b)] + e^2 - f^2\right\} F_0} \tag{41}$$

Forward Bending Moment Equation

The development of the general bending equation for the joint with intermediate contact relief would be similar to the preceding development for a joint with continuous contact as illustrated on Page 5. For the forward end of the joint, the distributed load, w_x, would be the same as in equation (9), the variable concentrated load, W_x, in terms of the distributed load, would be the same as in equation

(10), and the load center location $\bar{x}_x$, would be the same as in equation (13). At this point, however, to simplify the expressions of the bending moment equations for the joint with intermediate contact relief, the equations are expressed in terms of the maximum distributed loads, w_1 and w_2, in lieu of the concentrated loads, W_1 and W_2, as was done previously. The general expression for the bending moment at any location along the forward end of the joint with relief contact can be expressed as a combination of the moment attributed to the externally applied loads, M_0 and F_0, together with the product of the variable concentrated load, W_x, given in equation (10), and the distance to the load center location $\bar{x}_x$.

$$M_x = M_0 + F_0 x - W_x \bar{x}_x \quad \text{for } L - b \leq x \leq L - b + e$$

Substituting for W_x and $\bar{x}_x$ using equations (10) and (13) yields, after simplifying

$$M_x = M_0 + F_0 x - \frac{w_1}{6}\left[3(x-L+b)^2 - \frac{(x-L+b)^3}{(b-a-c)}\right] \quad \text{for } L-b \leq x \leq L-b+e \tag{42}$$

where w_1 and c are determined from equations (38) and (41).

Central Bending Moment Equation

Similarly the general expression for the bending moment at any location along the intermediate section of the joint with contact relief would be the sum of the product of a concentrated load, W_1, and the distance to the load center location, combined with the moment attributed to the externally applied loads M_0 and F_0

$$M_x = M_0 + F_0 x - W_1 (x - L + b - \bar{x}_1) \quad \text{for } L - b + e \leq x \leq L - a - f$$

Substituting for W_1, obtained by rearranging equation (38), and for $\bar{x}_1$, using equation (31) yields the following, after simplifying

$$M_x = M_0 + F_0 x - \left[\frac{w_1 e}{6(b-a-c)}\right]\left\{3(x-L+b)\left[2(b-a-c)-e\right] - e\left[3(b-a-c) - 2e\right]\right\}$$

$$\text{for } L - b + e \leq x \leq L - a - f \tag{43}$$

where w_1 and c are determined from equations (38) and (41).

Aft Bending Moment Equation

To obtain a general expression of the bending moment at any location along the aft end of the joint with contact relief, see adjacent figure, an expression for the variable concentrated load for the partial section, W_x, and its relative location, $\bar{x}_x$, are first needed. The variable concentrated load can be obtained by first using the properties of similar triangles to determine the magnitude of the distributed load at the end of the partial section, w_x'

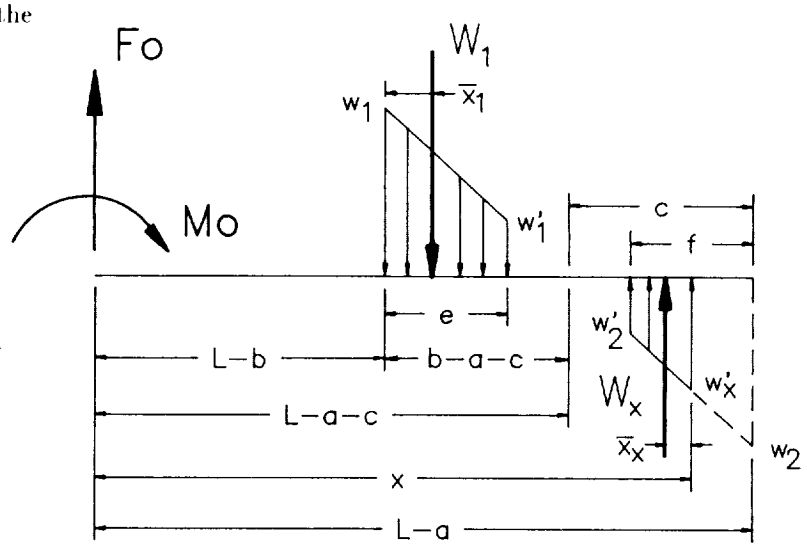

$$w'_x = \frac{w_2}{c}\,[x - (L - a - c)] \qquad \text{for } L - a - f \leq x \leq L - a \tag{44}$$

The variable concentrated load for the partial section would then simply be the product of the average of the distributed loads at the two ends times the length of the section

$$W_x = \left(\frac{w_2' + w'_x}{2}\right)(x - L + a + f) \qquad \text{for } L - a - f \leq x \leq L - a \tag{45}$$

substituting for w_2' and w_x', using equations (30) and (44), yields the desired expression for the concentrated load, after regrouping

$$W_x = \frac{w_2}{2c} (x - L + a + 2c - f) (x - L + a + f) \qquad \text{for } L - a - f \leq x \leq L - a \tag{46}$$

To obtain the relative location of this load, $\bar{x}_x$, a similar development that was used to determine the load centers $\bar{x}_1$ and $\bar{x}_2$, given in equations (27) and (28), can be used to provide the following expression for the relative location of the load

$$\bar{x}_x = \frac{(x - L + a + f)}{3} \left(\frac{w'_x + 2w_2'}{w_x' + w_2'} \right) \qquad \text{for } L - a - f \leq x \leq L - a \tag{47}$$

which after substituting for w_2' and w_x', using equations (30) and (44) yields, after simplifying

$$\bar{x}_x = \frac{(x - L + a + f)}{3} \left(\frac{x - L + a + 3c - 2f}{x - L + a + 2c - f} \right) \qquad \text{for } L - a - f \leq x \leq L - a \tag{48}$$

The general expression for the bending moment at any location along the aft end of the forward joint member of the joint with contact relief can now be expressed as the sum of the product of the variable concentrated load, W_x, and the distance to its respective load center, $\bar{x}_x$, in combination with the moment up through the intermediate section, as given in equation (42).

$$M_x = M_0 + F_0 x - W_1 (x - L + b - \bar{x}_1) + W_x \bar{x}_x \qquad \text{for } L - a - f \leq x \leq L - a$$

Substituting for W_x and $\bar{x}_x$, using equations (46) and (48) yields, after simplifying

$$M_x = M_0 + F_0 x - \left[\frac{w_1 e}{6(b-a-c)} \right] \left\{ 3(x-L+b) \left[2(b-a-c)-e \right] - e \left[3(b-a-c) - 2e \right] \right\} + \frac{w_2}{6c} (x - L + a + f)^2 (x - L + a + 3c - 2f) \qquad \text{for } L - a - f \leq x \leq L - a \tag{49}$$

where w_1, w_2, and c are determined from equations (38), (39) and (41).

BENDING MOMENT EQUATIONS FOR AFT JOINT MEMBER WITH INTERMEDIATE CONTACT RELIEF

As was done for the joint with continuous contact, the bending moment equations for the aft joint member can be obtained directly from the equations for the forward joint member by simply omitting terms that include the external load F_0 and M_0 and changing the sign of the remaining terms, see Figure 3c for an illustration of the loads.

The following general expression for the bending moment equations along the forward end of the aft joint member is obtained by revising equation (42).

$$M_x = \frac{w_1}{6}\left[3\,(x - L + b)^2 - \frac{(x - L + b)^3}{(b - a - c)}\right] \quad \text{for } L - b \le x \le L - b + e \tag{50}$$

where w_1 and c are determined from equations (38) and (41).

Revising equation (43) yields the general bending moment equation along the intermediate section of the aft joint member.

$$M_x = \frac{w_1 e}{6(b - a - c)}\{3(x - L + b)\,[2(b - a - c) - e] - e\,[3(b - a - c) - 2e]\} \tag{57}$$

$$\text{for } L - b + e \le x \le L - a - f$$

where w_1 and c are determined from equations (38) and (41).

The final expression is for the bending moment equation along the aft end of the aft joint member and was obtained by revising equation (49).

$$M_x = \frac{w_1 e}{6(b - a - c)} \{3(x - L + b)[2(b - a - c) - e] - e[3(b - a - c) - 2e]\}$$

$$- \frac{w_2}{6c}(x - L + a + f)^2 (x - L + a + 3c - 2f) \quad \text{for } L - b + e \leq x \leq L - a - f \tag{52}$$

where w_1, w_2 and c are determined from equations (38), (39) and (41).

JOINT STRESS RELATIONSHIPS

To evaluate the strength of a typical socket type joint of a model support system, the previously developed results can be combined with appropriate geometric properties to determine the respective stresses. The previously developed results were independent of the overall geometry of the joint, except for using the length of the joint for distributing the loadings, but for the following development of the stress equations, specific cross sectional shapes are needed. For the typical socket joints found in NASA LaRC wind tunnel model support systems, shown in Figure 4, a frustum of a cone would be representative of the geometry and is therefore used here to determine typical sectional properties. The resulting stresses are based on a force and moment such as a normal force and pitch moment and if other combined loads are to be considered simultaneously, such as a side force and yaw moment, results must be obtained vectorily. Results for joint geometries other than a frustrum of a cone can be developed similar to the following by substitution of appropriate sectional properties.

Bending Stress

Because of variations in geometry, the affect of the sectional properties interacting with the affect of the bending moment change along the length of the joint and the locations of the maximum bending stress and the maximum bending moment do not necessarily coincide, particularly for the first joint member as is illustrated in Figure 4. For the second joint member the bending moment is increasing as a function of "x" and generally the maximum stress occurs at the end of the joint where the bending moment is a maximum. The bending stress in either joint member can be evaluated from the following relationship

$$\sigma_b = \frac{M_x}{I/c} \tag{53}$$

where M_x is the respective bending moment, determined from the previously developed bending moment equations, and I/c is the section property at the cross section being evaluated. Note that for tapered joints, the cross-sectional properties vary along the length of the joint and the effect of this variation has to be considered concurrently with the changes in the bending moment in order to obtain the absolute maximum. Generally the maximum for the forward joint member occurs within the forward ten percent of the length, and for the aft joint members the maximum is at the aft end of the joint, but it is recommended that the relative bending stresses be evaluated iteratively at a sufficient number of locations to identify where the absolute maximum bending stress occurs.

Transverse Shear Stress

The maximum shear stress for each of the two joint members occurs at opposite ends of the respective joints and is where the full shear force is carried totally by only one of the beam members, see Figure 4. For the distribution through the cross section, the maximum occurs at the neutral axis with respect to bending flexure and for solid circular beam cross section the maximum shear stress would be as given in Reference 2

$$\tau = \frac{4V}{3A_s} = \frac{4F_0}{3A_s} \tag{54}$$

where the shear force, V, is equivalent to the externally applied force, F_0 and the area, A_s, is the sectional area of the respective joint member. For a hollow circular cross section the maximum would be similar

$$\tau = \frac{2V}{A_s} = \frac{2F_0}{A_s} \tag{55}$$

Note that the maximum shear stress, with respect to the distribution through the cross section, would be where the bending stress is zero and the maximum bending stress is where shear stress is zero so combining the maximum shear stress with the maximum bending stress is not necessary, see Reference 4 for further detail.

Hoop Stress

The hoop stress is an expression of how the peripheral tensile loads are carried tangentially in the wall of the outer joint member and is a result of the contact loads. Consider a section of the outer joint member sliced horizontally, and the hoop stress can be physically interpreted as the lateral forces that are tending to separate the joint along this section cut.

$$\sigma_h = \frac{p}{A_h} \tag{56}$$

Where the local lateral force in the joint, p, would be the product of a distributed load, w, and some differential length and the area of the material resisting this force would be the product of twice the wall thickness, 2t, to account for the two sides of the joint, multiplied by the same differential length as in the numerator. Rewriting the previous equation in terms of these definitions and canceling the differential length from both the numerator and the denominator yields

$$\sigma_h = \frac{w}{2t} \tag{57}$$

Note that both the distributed load, w, and the wall thickness, t, vary along the length of the joint and although generally the maximum occurs at the free end of the outer joint member, for w_1 as given in either equation (4) or equation (38), it is best to at least spot check some other locations to verify that the thinner wall sections do not result in an even larger stress. The equation is valid along the length of the entire joint and can be used to evaluate the local hoop stress at any location along the length of the joint by simply using the appropriate distributed load together with the corresponding wall thickness at the same respective location.

Contact Pressure Stress

The previously developed expressions were for the linear distribution along the length of the joint and to obtain a true distribution of the contact loads a lateral distribution across the width of the joint is needed. In general for elastic, curved bodies that are in compression, an elliptic load distribution is assumed that considers mutual deflections between the contacting bodies. To obtain the maximum contact pressure stress, also known as the Hertz contact stress, the elliptical load distribution can be

integrated over the width of the joint and the result then solved for the maximum. The integral can be set up by using the maximum pressure as one of the parameters in the equation of an ellipse to determine the limits of integration. Setting up the integral and integrating yields an expression for the linear distributed load in terms of the maximum pressure

$$w = \int_{-r}^{+r} \frac{P_{max}}{r} \sqrt{r^2 - z^2}\, dz = \frac{P_{max}}{2r}\left[\sqrt{z\ r^2 - z^2} + r^2 \sin^{-1}\frac{z}{r}\right]_{-r}^{+r} = \frac{\pi r P_{max}}{2} \tag{58}$$

Solving this expression for the maximum contact pressure, P_{max}, in terms of the local joint diameter of the contacting surfaces, d, and linear distributed load, w, provides the desired expression for the maximum bearing stress between the mating surfaces of the joint members which is equivalent to the maximum contact pressure

$$\sigma_p = P_{max} = \frac{4w}{\pi d} \tag{59}$$

For a tapered joint, the maximum can occur at either end of the joint, depending on the worse case combination of the distributed loads w_1 and w_2, as determined from either equations (4), (5), (38) and (39) and the local diameter of the contacting surfaces, d. Note that the bearing stress acts in the radial direction and actually can only exists where the joint members are in contact.

CONCLUSION

The results included in this report were originally developed to evaluate the stresses in concentric, tapered, socket type joints for wind tunnel model support systems and the stress equations included in this report reflect this application. Although the analysis was for a specific geometry, the method is applicable to other joints as shown in Figure 1 and discussed in the Introduction. As pointed out in the Introduction, the key feature of this method was that the loading be transferred from one joint member to the other by the mutual contact pressure between the joint members and that the distribution vary linearly along the length of the joint from some maximum at one end to a minimum at the other end. The assumed linear load distribution of the contact pressure would be applicable to other configurations, because the Strength of Materials principles used in the analysis is independent of the geometry, but the stress equations would depend on a specific geometry and may need to be revised for new geometries of different configurations. The expressions for the distributed loads and bending moments included in this report can be used to develop new bearing pressure and stress equations for other geometries by simply substituting the appropriate sectional properties for any new geometry. In general, the development of new stress equations for different geometries would be similar to the development of the included stress equations and the only differences would be attributed to the differences due to the new sectional properties. A restriction that must be considered when developing new pressure/stress relationships is that the geometry of the joint must consist of an overlapping arrangement of the joint members such that the loads transfer from one joint member to the other solely by the mutual contact pressure. Any attachments to the joint that can alter the assumed linear load distribution such as threaded draw nuts would affect the computed results and the use of this analytical technique would then not be applicable for such configurations.

To verify the assumption of linearity in the load distribution, a finite element analysis was performed, see Appendix B. A finite element model of a typical joint from a wind tunnel model support system in the National Transonic Facility was generated complete with loads that are typical of a representative model. To study the effect of differences in the relative bending stiffnesses of the joint members the thickness of the outer joint member was varied with two subsequent finite element models. The reference configuration was modified to generate two new finite element models, one with a thicker outer joint member and one with a thinner outer joint member, but the dimensions of the inner joint member was the same in all the finite element models. The results of the finite element analysis

indicate the calculated results from using the equations in this report would be conservative for the range of variations in the thickness of the joint members considered. It should be noted, however, that the best calculated results would be obtained when the stiffness of the outer joint member is a couple of orders of magnitude greater than the stiffness of the inner joint member.

With regard to an appropriate aspect ratio for the length to diameter of the contacting surfaces of the joint members, consider the joints illustrated in Appendix B. For the joints that were analyzed, the aspect ratio was slightly less than two, based on the larger diameter of the inner joint member and the contact length of the joint members. If the aspect ratio is much smaller than two, the inner joint member will physically tend to rotate within the outer joint member and increase the concentrated loads at each end of the joint. If the aspect ratio is much larger than two, the actual load distribution would tend to decrease basically exponentially toward the small end of the inner joint member and the small end of the inner joint member would not carry its fair share of the load. Neither of these effects can be evaluated from the results in this report, since the loads were assumed to vary linearly, and as a general rule it is recommended that the aspect ratio be kept as close to two as possible to avoid any needless problems.

In general, the calculated results obtained from using the equations in this report are considered to be conservative but relatively coarse. If a more complete description of the stress state in the joint is desired, it is suggested that a more detailed analytical method such as finite element analysis be used. The results presented in this report were not intended to replace the need for more detailed analytical methods but instead, the results are considered acceptable for use in conservatively evaluating the strength of joints in new model support systems.

APPENDIX A

IBM BASIC PROGRAM

```
100 REM  Latest program revision:  August 14, 1984.
110 REM
120 REM  Program computes Joint Loads and Stresses in Socket-type joints
130 REM  that have a circular cross section.  For additional detail refer
140 REM  to "Contact Loads and Stresses in Socket Type Joints", Wyle
150 REM  Report WSA02.1-NTF, by L.C.Rash, Dec.22,1983.
160 REM
170 REM  Program computes bending moments and stresses only for the
180 REM  length of engagement of the joint.  For a joint with relief the
190 REM  number of computations would be 3(N+1) and for no relief they
200 REM  would be (N+1), where N is the input "No. of divisions".  For
210 REM  additional bending calculations, a restart option is available
220 REM  at the end of the program to allow entering a new value of N.
230 REM
240 REM  Program is adaptable to tapered or nontapered joints that may or
250 REM  may not have surface relief:
260 REM    * The respective taper is established by entering the inside
270 REM      diameters, Di, mean diameters, Dm, and outside diameters, Do,
280 REM      for both ends of the joint (end 1 is near the loads and end 2
290 REM      is near the support).  If Dm1 and Dm2 are equal, the program will
300 REM      ask for the Beam No. of the male joint member, otherwise the
310 REM      program determines the respective joint type from the geometries.
320 REM    * The surface relief is the magnitude that the radius is to be
330 REM      decreased and is defined by entering the depth,R, and the distance
340 REM      from the ends, e & f, where the relief is to start and stop.
350 REM
360 PRINT "PROGRAM TO COMPUTE LOADS AND STRESSES IN CIRCULAR JOINTS"
370 PRINT
380 DEFDBL A-Z
390 PRINT "Enter date and Problem Description (commas not allowed)"
400 INPUT PRB$
410 PRINT "Enter No. of divisions.   (Controls number of bending calculations)"
420 INPUT N
430 IF N<=.99 THEN N=1
440 PRINT"Enter depth of surface relief (in).        (0 if none)"
450 INPUT R
460 IF R=>.00001 GOTO 520
470 E=0#
480 F=0#
490 PRINT "Enter dimensions: l-a, l-b (in)    (Socket Joint with NO relief)"
500 INPUT LA,LB
510 GOTO 540
520 PRINT "Enter dimensions: l-a, l-b, e, f (in)   (Socket Joint with Relief)"
530 INPUT LA,LB,E,F
540 PRINT "Enter joint diameters : Di, Dm, Do (in)    (location 1: near loads)"
550 INPUT DI1,DM1,DO1
560 PRINT "Enter joint diameters : Di, Dm, Do (in)  (location 2: near support)"
570 INPUT DI2,DM2,DO2
580 IF DM1<DM2 THEN BM=2: GOTO 600
590 BM=1
600 IF ABS(DM1-DM2)<.001 THEN PRINT "Enter Beam No. of male joint member":INPUT
BM
610 PRINT "Enter loads:  Fo (lbs), Mo (in-lbs)"
620 INPUT FO,MO
630 IF R<.00001 GOTO 800
640 REM  Calculate Load Reversal Location     (Joint with relief)
650 BA=LA-LB
660 CM=2*E*BA+F^2-E^2
670 CF=LA*F^2-2*(F^3+E^3)/3+(BA-LB)*E^2+2*BA*LB*E
680 CD=2*(E+F)*MO+(2*(F*LA+E*LB)+E^2-F^2)*FO
```

```
690 C=(CM*MO+CF*FO)/CD
700 REM  Calculate Joint Loads      (Joint with relief)
710 BAC=BA-C
720 E3=(E/3)*(3*BAC-2*E)/(2*BAC-E)
730 F3=(F/3)*(3*C-2*F)/(2*C-F)
740 W1=(MO+(LA-F3)*FO)/(BA-E3-F3)
750 W2=(MO+(LB+E3)*FO)/(BA-E3-F3)
760 W1PL=(2*W1/E)*(BAC/(2*BAC-E))
770 W2PL=(2*W2/F)*(C/(2*C-F))
780 GOTO 890
790 REM C-location and Loads (Joint with NO relief)
800 BA=LA-LB
810 MF=MO+FO*LA
820 C=(3*BA*MF-2*FO*BA^2)/(6*MF-3*BA*FO)
830 W1=(3*MF-C*FO)/(2*BA)
840 W2=(3*MF-(C+2*BA)*FO)/(2*BA)
850 BAC=BA-C
860 W1PL=2*W1/BAC
870 W2PL=2*W2/C
880 REM  Calculate Hoop and Pressure Stresses
890 PI=3.141592654#
900 C!=C
910 HP1!=W1PL/(DO1-DM1)
920 HP2!=W2PL/(DO2-DM2)
930 PR1!=-4*W1PL/(PI*DM1)
940 PR2!=-4*W2PL/(PI*DM2)
950 W1!=W1
960 W2!=W2
970 W1PL!=W1PL
980 W2PL!=W2PL
990 PRINT
1000 PRINT
1010 PRINT PRB$
1020 PRINT
1030 IF R<.00001 GOTO 1060
1040 PRINT "  ANALYSIS OF SOCKET TYPE JOINT WITH INTERMEDIATE SURFACE RELIEF"
1050 GOTO 1070
1060 PRINT "      ANALYSIS OF SOCKET TYPE JOINT WITH CONTINUOUS CONTACT"
1070 PRINT "-----------------------------------------------------------------"
1080 PRINT "      Joint Dimensions:     l-a =" LA"in"
1090 PRINT "                            l-b =" LB"in"
1100 PRINT "                            b-a =" BA"in"
1110 IF R<.00001 GOTO 1150
1120 PRINT "                              e =" E"in"
1130 PRINT "                              f =" F"in"
1140 PRINT "                         Relief =" R"in"
1150 PRINT
1160 PRINT "      Joint Diameters:        Di =" DI1"in"
1170 PRINT "      (at location 1)         Dm =" DM1"in"
1180 PRINT "                              Do =" DO1"in"
1190 PRINT
1200 PRINT "      Joint Diameters:        Di =" DI2"in"
1210 PRINT "      (at location 2)         Dm =" DM2"in"
1220 PRINT "                              Do =" DO2"in"
1230 PRINT
1240 PRINT "      Applied Loads:       Force =" FO"lbs"
1250 PRINT "                          Moment =" MO"in-lbs"
1260 PRINT "-----------------------------------------------------------------"
1270 PRINT "         Load Reversal Location =" C!"in    (from location 2)"
1280 PRINT " Equivalent Concentrated Load 1 =" W1!"lbs"
```

```
1290 PRINT " Equivalent Concentrated Load 2 =" W2!"lbs"
1300 PRINT "              Distributed Load 1 =" W1PL!"lbs/in"
1310 PRINT "              Distributed Load 2 =" W2PL!"lbs/in"
1320 PRINT "-----------------------------------------------------------------"
1330 PRINT "    Hoop Stress (at location 1) =" HP1!"psi"
1340 PRINT "    Hoop Stress (at location 2) =" HP2!"psi"
1350 PRINT
1360 PRINT "Pressure Stress (at location 1) = " PR1!"psi"
1370 PRINT "Pressure Stress (at location 2) = " PR2!"psi"
1380 PRINT "-----------------------------------------------------------------"
1390 PRINT "                  BEAM # 1 (BENDING)          BEAM # 2 (BENDING)"
1400 PRINT "  X,in       MOMENT,in-lbs  STRESS,psi   MOMENT,in-lbs  STRESS,psi
1410 IF R<.00001 GOTO 2140
1420 PRINT
1430 REM Initializing x-variables    (Joint with relief)
1440 X=LB
1450 DX1=E/N
1460 DX2=(BA-E-F)/N
1470 DX3=F/N
1480 XLB=X-LB
1490 X!=X
1500 REM  Determine relative diameters     (Joint with relief)
1510 DIX=DI1+(DI2-DI1)*XLB/BA
1520 DMX=DM1+(DM2-DM1)*XLB/BA
1530 DOX=DO1+(DO2-DO1)*XLB/BA
1540 DRX=DMX-2*R
1550 REM  Determine relative Section Properties     (Joint with relief)
1560 ICI=PI*(DMX^4-DIX^4)/(32*DMX)
1570 ICO=PI*(DOX^4-DMX^4)/(32*DOX)
1580 ICR=PI*(DRX^4-DIX^4)/(32*DRX)
1590 REM  Calculate Bending Moments     (Joint with relief)
1600 LBE=LB+E
1610 LAF=LA-F
1620 IF X>LBE GOTO 1650
1630 MX2=(W1PL/6)*(3*XLB^2-(XLB^3)/BAC)
1640 GOTO 1690
1650 MX2=(3*XLB*(2*BAC-E)-E*(3*BAC-2*E))*W1PL*E/(6*BAC)
1660 IF X>LAF GOTO 1680
1670 GOTO 1690
1680 MX2=MX2-(X-LA+F)^2*(X-LA+3*C-2*F)*W2PL/(6*C)
1690 MX1=MO+FO*X-MX2
1700 MX1!=MX1
1710 MX2!=MX2
1720 IF MX1!<.001, THEN MX1!=0!
1730 IF MX2!<.001, THEN MX2!=0!
1740 IF ((BM-1.5)>.001) GOTO 1920
1750 REM Calculate Bending Stresses for Dm1 > Dm2     (Joint with relief)
1760 BDG1!=MX1/ICI
1770 BDG2!=MX2/ICO
1780 BDG3!=MX1/ICR
1790 IF BDG1!<.0001, THEN BDG1!=0!
1800 IF BDG2!<.0001, THEN BDG2!=0!
1810 IF BDG3!<.0001, THEN BDG3!=0!
1820 REM  Print Bending Moments and Stresses for Dm1>Dm2    (Joint with relief)
1830 IF (LBE-X)>.00001, THEN PRINT X!,MX1!,BDG1!,MX2!,BDG2!
1840 IF ABS(LBE-X)<=.0001, THEN PRINT X!,MX1!,BDG1!,MX2!,BDG2!
1850 IF ABS(LBE-X)<=.0001, THEN PRINT: PRINT X!,MX1!,BDG3!,MX2!,BDG2!
1860 IF ((X-LBE)>.0001) AND ((LAF-X)>.0001) THEN PRINT X!,MX1!,BDG3!,MX2!,BDG2!
1870 IF ABS(LAF-X)<=.0001, THEN PRINT X!,MX1!,BDG3!,MX2!,BDG2!
1880 IF ABS(LAF-X)<=.0001, THEN PRINT: PRINT X!,MX1!,BDG1!,MX2!,BDG2!
```

```
1890 IF ((X-LAF)>.0001) AND ((X-LA)<.0001) THEN PRINT X!,MX1!,BDG1!,MX2!,BDG2!
1900 GOTO 2070
1910 REM Calculate Bending stresses for Dm1 < Dm2     (Joint with relief)
1920 BDG1!=MX1/ICO
1930 BDG2!=MX2/ICI
1940 BDG3!=MX2/ICR
1950 IF BDG1!<.0001, THEN BDG1!=0!
1960 IF BDG2!<.0001, THEN BDG2!=0!
1970 IF BDG3!<.0001, THEN BDG3!=0!
1980 REM  Print Bending Moments and Stresses for Dm1<Dm2    (Joint with relief)
1990 IF (LBE-X)>.00001, THEN PRINT X!,MX1!,BDG1!,MX2!,BDG2!
2000 IF ABS(LBE-X)<=.0001, THEN PRINT X!,MX1!,BDG1!,MX2!,BDG2!
2010 IF ABS(LBE-X)<=.0001, THEN PRINT: PRINT X!,MX1!,BDG1!,MX2!,BDG3!
2020 IF ((X-LBE)>.0001) AND ((LAF-X)>.0001) THEN PRINT X!,MX1!,BDG1!,MX2!,BDG3!
2030 IF ABS(LAF-X)<=.0001, THEN PRINT X!,MX1!,BDG1!,MX2!,BDG3!
2040 IF ABS(LAF-X)<=.0001, THEN PRINT: PRINT X!,MX1!,BDG1!,MX2!,BDG2!
2050 IF ((X-LAF)>.0001) AND ((X-LA)<.0001), THEN PRINT X!,MX1!,BDG1!,MX2!,BDG2!
2060 REM  Incrementing x-variable and restarting     (Joint with relief)
2070 IF((LBE-X)>.0001), THEN X2=X+DX1
2080 IF ((LBE-X)<=.0001) AND ((X-LAF)<.0001), THEN X2=X+DX2
2090 IF ((LAF-X)<=.0001), THEN X2=X+DX3
2100 IF ((X-LA)>.1) GOTO 2510
2110 X=X2
2120 GOTO 1480
2130 REM  Initializing x-variable     (Joint with NO relief)
2140 X=LB
2150 DX=BA/N
2160 XLB=X-LB
2170 X!=X
2180 REM  Determine relative diameters     (Joint with NO relief)
2190 DIX=DI1+(DI2-DI1)*XLB/BA
2200 DMX=DM1+(DM2-DM1)*XLB/BA
2210 DOX=DO1+(DO2-DO1)*XLB/BA
2220 REM  Determine relative Section Properties     (Joint with NO relief)
2230 ICI=PI*(DMX^4-DIX^4)/(32*DMX)
2240 ICO=PI*(DOX^4-DMX^4)/(32*DOX)
2250 REM  Calculate Bending Moments     (Joint with NO relief)
2260 IF XLB>BAC GOTO 2290
2270 MX2=(W1/3)*(3*XLB^2/BAC-XLB^3/(BAC^2))
2280 GOTO 2300
2290 MX2=(W1/3)*(3*X-2*LB-LA+C)-(W2/3)*(X-LA+C)^3/(C^2)
2300 MX1=MO+FO*X-MX2
2310 MX1!=MX1
2320 MX2!=MX2
2330 IF MX1!<.001 THEN MX1!=0!
2340 IF MX2!<.001 THEN MX2!=0!
2350 IF ((BM-1.5)>.001) GOTO 2410
2360 REM Calculate Bending Stress for Dm1 < Dm2     (Joint with NO relief)
2370 BDG1!=MX1/ICI
2380 BDG2!=MX2/ICO
2390 GOTO 2430
2400 REM Calculate Bending Stress for Dm1 > Dm2     (Joint with NO relief)
2410 BDG1!=MX1/ICO
2420 BDG2!=MX2/ICI
2430 IF BDG1!<.001 THEN BDG1!=0!
2440 IF BDG2!<.001 THEN BDG2!=0!
2450 PRINT X!,MX1!,BDG1!,MX2!,BDG2!
2460 REM  Incrementing x-variable and restarting     (Joint with NO relief)
2470 X=X+DX
2480 IF ((X-LA)>.1) GOTO 2510
```

```
2490 GOTO 2160
2500 REM  Concludes bending calculations for both types of joints
2510 PRINT "-----------------------------------------------------------------"
2520 PRINT
2530 PRINT "To restart bending calcs., re-enter No. of divisions (0 to stop)"
2540 INPUT N
2550 PRINT
2560 IF ((N-.999)>.0001) GOTO 1380
2570 END
```

APPENDIX B
VALIDATION OF LOADING WITH FINITE ELEMENTS

A finite element analysis, FEA, was performed to validate the profile of the assumed load distribution that was used in the socket joint analysis of this report. The results of the FEA were correlated with the linear variation in the load distribution, that was the premise of the analytical approach in evaluating the strength of socket joints, to demonstrate that the assumed load distribution provides conservative results. In order to show the interrelated effect of the relative stiffness of the respective joint members on the load distribution, three different joint configurations were independently evaluated with FEA. This evaluation was accomplished by increasing and decreasing the outer wall thickness from a reference configuration and then comparing the FEA results of all three configurations to the assumed linear variation in the load distribution.

The finite element model, FEM, that was developed as a reference for the analysis was representative of a typical socket joint found in NASA LaRC wind tunnel model support systems at the National Transonic Facility. The FEM is shown in Figure 5 and represents the joint between a two inch diameter balance, the inner joint member, and a three inch diameter sting, the outer joint member. This was the same balance and sting joint that was included as a Sample Problem for illustrating the analytical results in Reference 1. The FEM consisted of three dimensional "brick" elements that were used to generate a symmetric half-model that included 2291 nodes and 1548 3-D elements. The loads for the FEM were the design loads of the balance from the Sample Problem: a 6500 lb normal force and a 13000 in-lb pitch moment acting at a location equivalent to the moment center of the balance. Nonlinear FEA results were equivalent to the moment center of the balance. Nonlinear FEA results were obtained by iterating with the FEM manually until only compressive reactions were obtained at the interface of the inner and outer joint members. To obtain these nonlinear results, the connectivity of the inner and outer joint members had to be released at any location where tensile type reactions were found, reconnected for any previously released location where the inner and outer joint members were found to overlap, and the FEA rerun until only compressive reactions were obtained with no overlapping of the joint members. Overlapping was detected by comparing the static deflection results from the FEA to see if the final

deformed position of either the inner and outer joint member extended across the geometric boundary of the other member. This overlapping condition could occur if connectivity was required at a location that had previously been released, due to a shift in the load distribution, and would allow a compressive load to once again be developed at that location. Once a solution was obtained that included only compressive loads or separation between the inner and outer joint members, the FEA results were accepted and the results were correlated to the profile of the distributed load that was assumed in the socket joint analysis.

The iterative process that was required to obtain a nonlinear solution had to be repeated for each of the three different configurations because the differences in the thicknesses of the outer joint member produced variations in the distribution of the compressive reactions that had to be considered independently. The results of the FEA for each configuration are shown in Figure 6 and include load distributions and illustrations of each of the three joint configurations. At the center of the figure is the reference configuration, taken from Reference 1, and at the top and bottom are the configurations for decreasing and increasing, respectively, the wall thickness of the outer joint member. The FEM that was based on the reference configuration was developed first and then copies of the input data file were modified to develop the FEMs of the other configurations. The other configurations that were selected to study the effects of variations in the wall thickness of the outer joint member on the load distribution were obtained by decreasing the diameter of the outer joint member to 2.25 inches for one FEM and by increasing the diameter of the outer joint member to 4.0 inches for another FEM. The inner joint member was kept the same for all three configurations. Key dimensions of each configuration and the resulting load distributions are shown in Figure 6.

To transform the radial reactions obtained from the FEA into equivalent vertical loads and to perform validations of the FEA results, a computer program was developed. The computer program not only provided tabulated results that could be directly compared to the distributed loads but also allowed complete equilibrium checks to readily be performed that provided confidence in the data obtained from the FEA. The reactions obtained from the FEA were normal to the surface between the inner and the outer joint members and the computer program transformed these reactions into vertical, lateral, and axial components. The distribution of the vertical components about the perimeter were lumped at the centerline, the lateral components were matched by the mirror image loads, and the

axial components were counterbalanced with loads equivalent to those developed by the locking devices that secure the balance to the sting. Also the sum of the vertical components was in equilibrium with the externally applied normal force and the sum of the moments of the vertical components and the

axial components about the equivalent moment center location was in equilibrium with the externally applied pitch moment. The vertical components that were lumped along the centerline are plotted in Figure 6 adjacent to the illustrations of the three joint configurations. The equivalent loads obtained from applying the results of the linearly distributed load obtained from the socket joint analysis, as in the Sample Problem of Reference 1, are also included for comparison.

A physical interpretation that illustrates the relative effect of the wall thickness would be to consider the thinner outer joint member as a thin wall tube and the corresponding inner joint member as basically a stiff round bar. As the load is applied, the contact loads near the end of the inner rod, the loads would be more concentrated at the end of the inner rod, and eventually lead to a failure mode of the inner rod punching through the thinner outer joint member. This is depicted by a sharp spike as shown on the right hand side of Figure 6a which is for the distributed load for the joint with thin outer member. For the thicker outer joint member, the thick wall would act more like a rigid support that would in effect be like cantilevering the inner joint member from the end of the outer joint member. The loads would be more concentrated at the end of the outer joint member and would tend to be more uniformly distributed near the end of the inner joint member. This is depicted by the sharp spike shown on the left hand side of Figure 6c which is for the distributed load for the joint with thick outer member. Note the similarity between the distributions is turned upside down and rotated end for end. The similarity in the distributions could be interpreted for the thinner outer joint member as the outer joint member is being cantilevered off of the end of the more rigid inner joint member and for the thicker outer joint member, as the inner joint member is being cantilevered off of the end of the more rigid outer joint members.

APPENDIX C

LIST OF SYMBOLS

a	reference dimension to aft end of joint
A_h	effective hoop stress area
A_s	effective shear stress area
b	reference dimension to forward end of joint
c	reference dimension to load reversal location
d	general diameter of joint member
dz	differential length for integral
e	reference length of forward contact surface
f	reference length of aft contact surface
F_0	externally applied force
I/c	bending section modulus
L	reference length of model support system
M_0	externally applied moment
M_x	variable bending moment
p	local lateral force in joint
P_{max}	maximum contact pressure
r	general radius of joint member
t	wall thickness of outer joint member
V	shear force
W_1	concentrated load equivalent to distributed load at forward end of joint
W_2	concentrated load equivalent to distributed load at aft end of joint
W_x	variable concentrated load equivalent to partially distributed load
w	general distributed load
w_1	maximum magnitude of distributed load at forward end of joint
w_1'	magnitude of distributed load at forward end of contact relief
w_2	maximum magnitude of distributed load at aft end of joint
w_2'	magnitude of distributed load at aft end of contact relief
w_x	magnitude of distributed load at section being evaluated
x	variable distance between external loads and section being evaluated
$\bar{x}_1$	load center location for forward end of joint
$\bar{x}_2$	load center location for aft end of joint
$\bar{x}_x$	variable load center location for partially distributed load
z	general circular coordinate
σ_b	bending stress
τ	shear stress
σ_h	hoop stress
σ_p	bearing pressure/stress

REFERENCES

1.) Rash, L.C., "Contact Loads and Stresses in Socket Type Joints", Wyle Laboratory Report WAS02.1-NTF, 1983

2.) Shigley, J.E., Mechanical Engineering Design, McGraw-Hill Book Company, 1963

3.) Roark, R. J., Formulas for Stress and Strain, McGraw Hill Book Company, 1965

4.) Popov, E.P., Introduction to Mechanics of Solids, Prentice-Hall, Inc., 1968

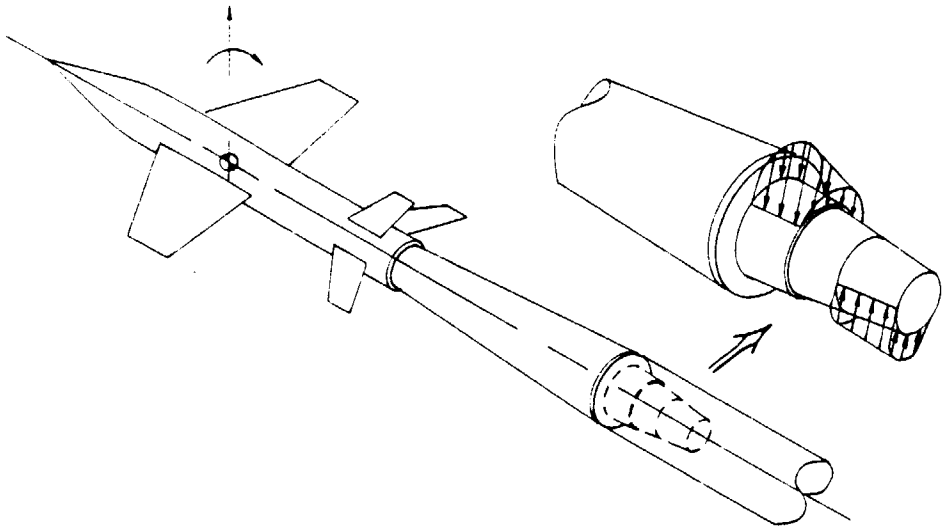

(a) A Sliding Tapered Joint in a Wind Tunnel Model Support System

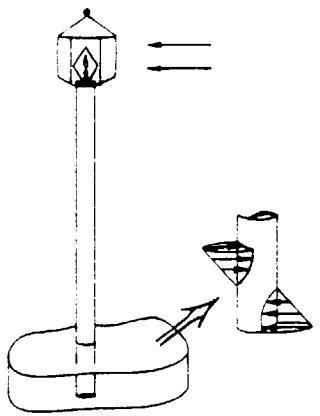

(b) A Lamppost in a Footing

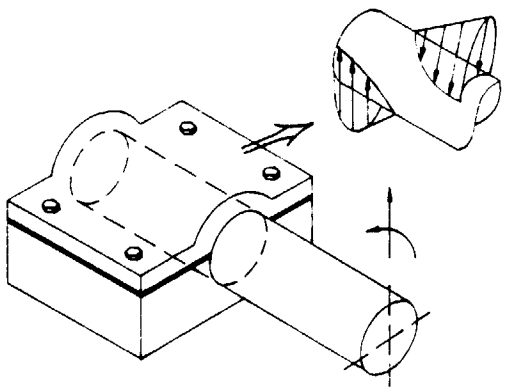

(c) A Round Bar in a Clamping Fixture

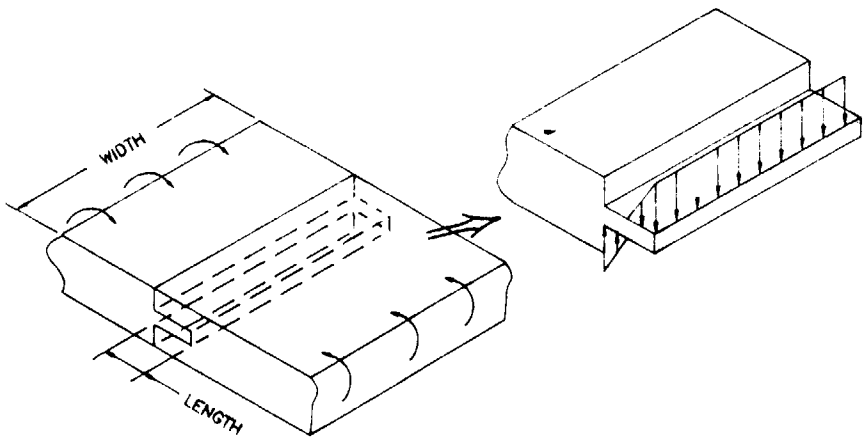

(d) A Tongue and Groove Joint (Width >> Length)

Figure 1. Typical Socket Type Joints

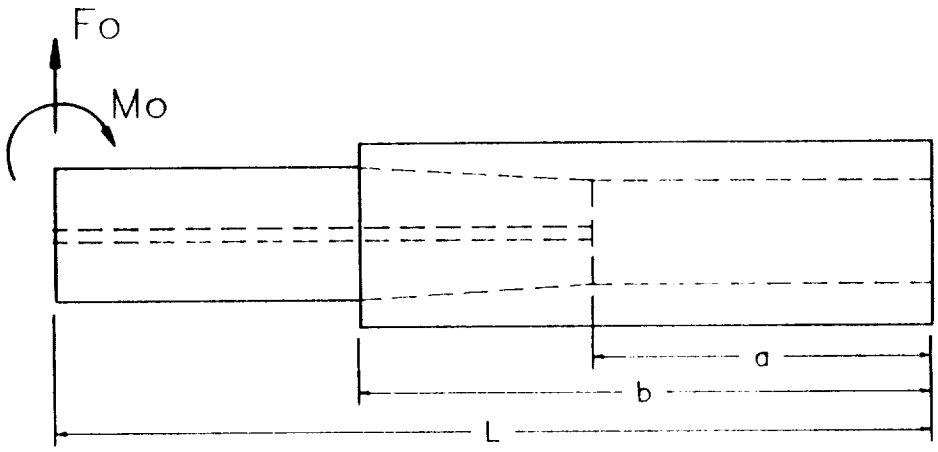

(a.) Typical Joint

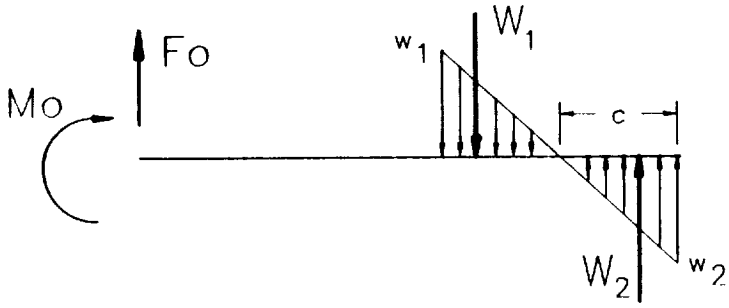

(b.) Loading Diagram of Fwd Joint Member

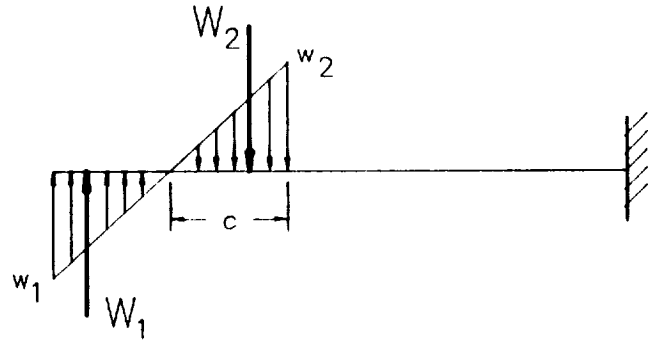

(c.) Loading Diagram of Aft Joint Member

Figure 2. Illustration of Socket Joint with Continuous Contact

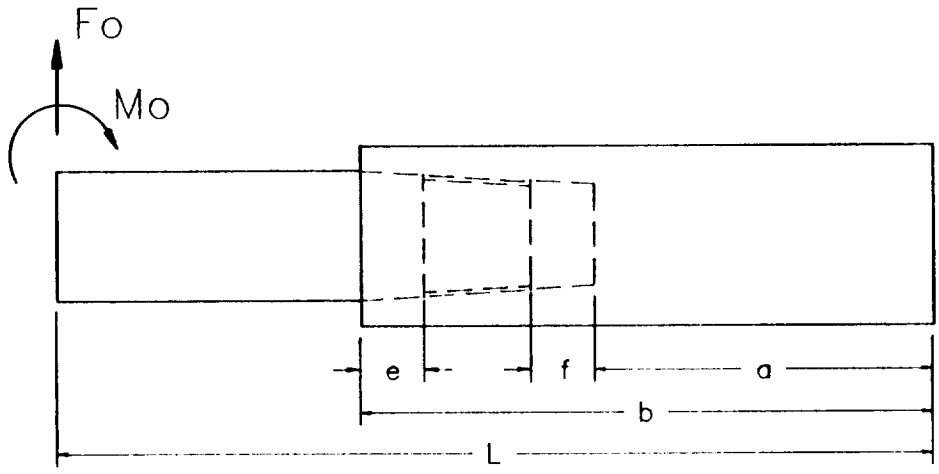

(a.) Typical Joint

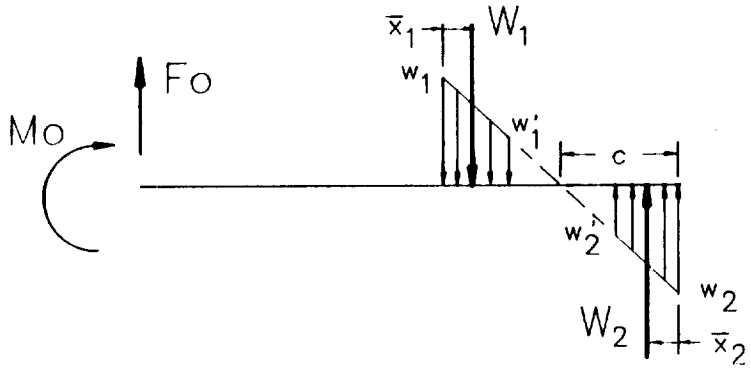

(b.) Loading Diagram of Fwd Joint Member

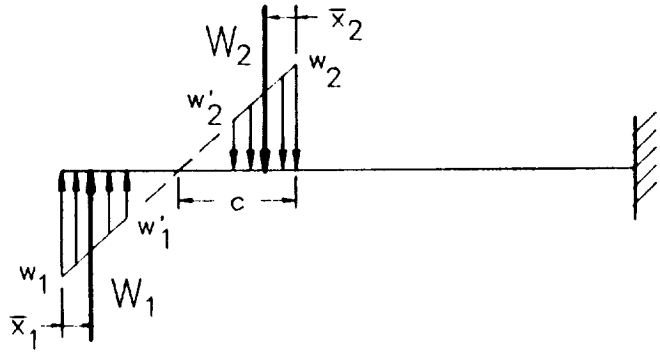

(c.) Loading Diagram of Aft Joint Member

Figure 3. Illustration of Socket Joint with Intermediate Contact Relief

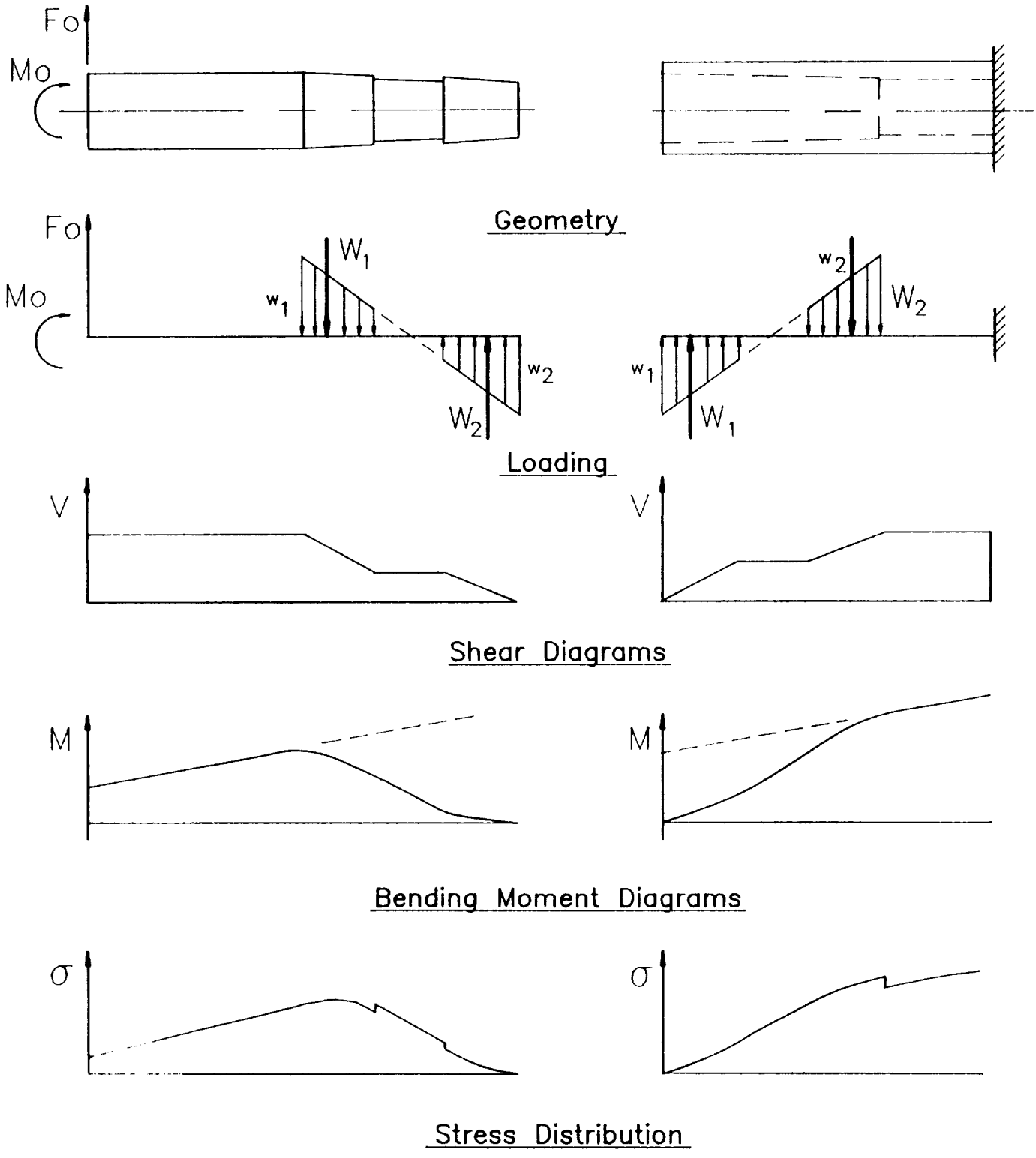

Figure 4. Typical Socket Joint Loadings and Results

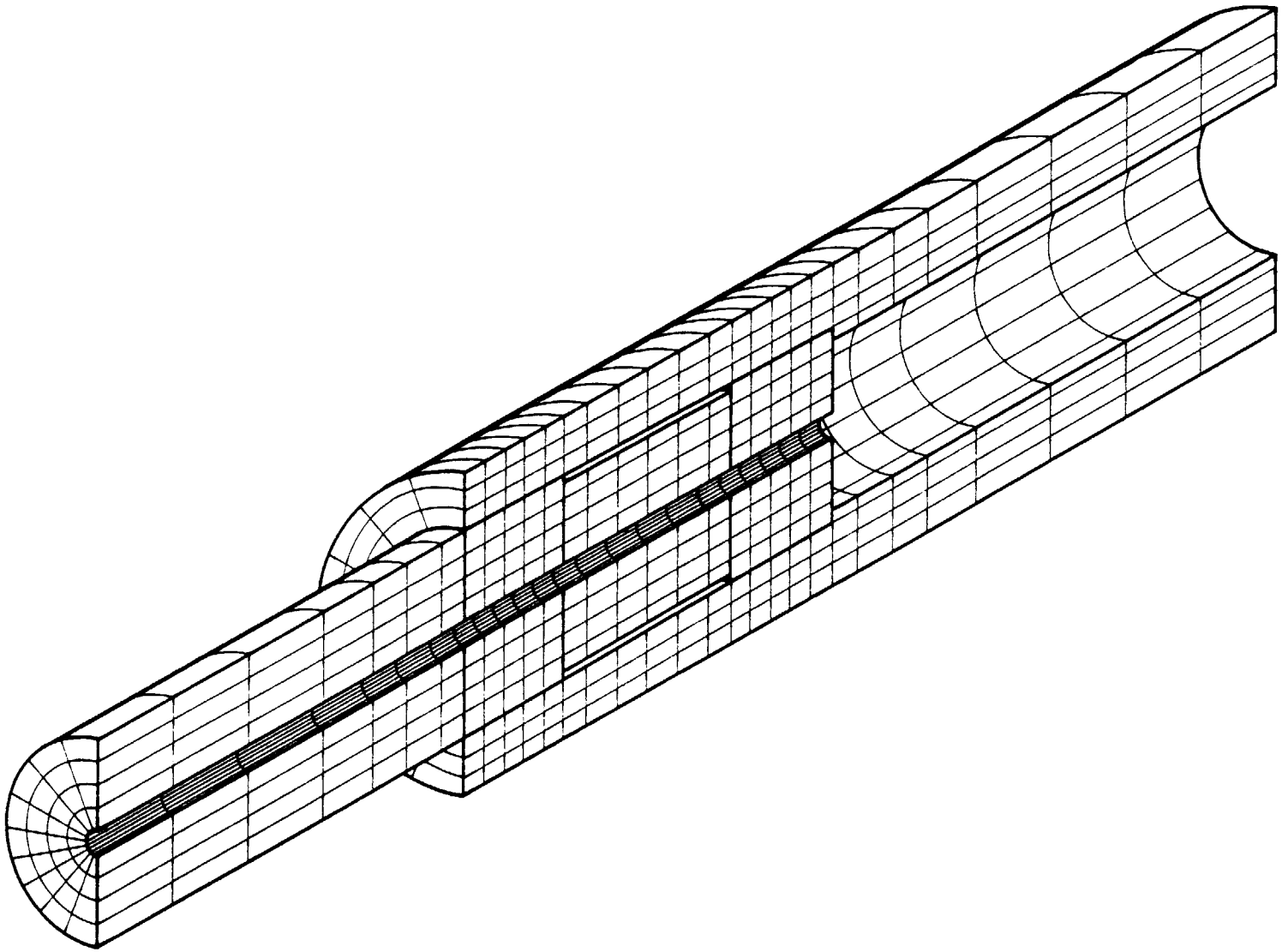

Figure 5. Finite Element Model of Socket Joint

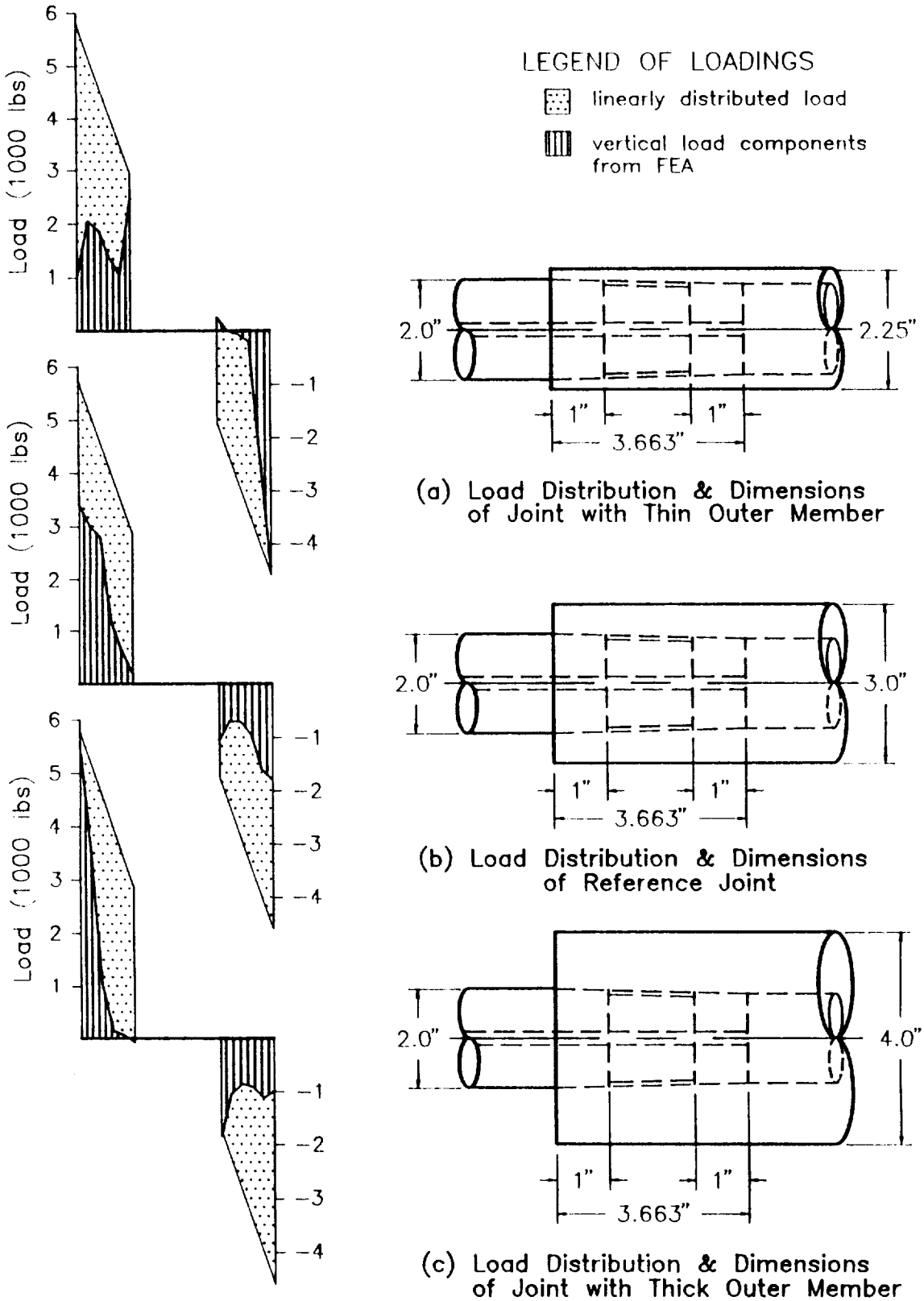

Figure 6. Load Distributions Resulting from FEA

REPORT DOCUMENTATION PAGE

Form Approved
OMB No. 0704-0188

1. AGENCY USE ONLY *(Leave blank)*	2. REPORT DATE	3. REPORT TYPE AND DATES COVERED
	June 1994	Contractor Report

4. TITLE AND SUBTITLE
Strength Evaluation of Socket Joints

5. FUNDING NUMBERS
C NAS1-19385

WU 505-59-85-01

6. AUTHOR(S)
Larry C. Rash

7. PERFORMING ORGANIZATION NAME(S) AND ADDRESS(ES)
Calspan Corporation
110 Mitchell Blvd.
Tullahoma, TN 37388

8. PERFORMING ORGANIZATION REPORT NUMBER

9. SPONSORING / MONITORING AGENCY NAME(S) AND ADDRESS(ES)
National Aeronautics and Space Administration
Langley Research Center
Hampton, VA 23681-0001

10. SPONSORING / MONITORING AGENCY REPORT NUMBER
NASA CR-4608

11. SUPPLEMENTARY NOTES
Langley Technical Monitor: Lawrence E. Putnam
Final Report

12a. DISTRIBUTION / AVAILABILITY STATEMENT
Unclassified - Unlimited

Subject Category 08

12b. DISTRIBUTION CODE

13. ABSTRACT ***(Maximum 200 words)***

This report documents the development of a set of equations that can be used to provide a relatively simple solution for identifying the strength of socket joints and for most cases avoid the need of more lengthy analyses. The analytical approach was verified by comparison of the contact load distributions to results obtained from a finite element analysis. The contacting surfaces for the specific joint in this analysis are in the shape of frustrums of a cone, and is representative of the tapered surfaces in the socket-type joints used to join segments of model support systems for wind tunnels. The results are in the form of equations that can be used to determine the contact loads and stresses in the joint from the given geometry and externally applied loads. Equations were determined to define the bending moments and stresses along the length of the joints based on Strength and Materials principles. The results have also been programmed for a personal computer and a copy of the program that was developed is included.

14. SUBJECT TERMS	15. NUMBER OF PAGES
Strength, Socket Joints, Model Support Systems, Wind Tunnel Models	44
	16. PRICE CODE: A03

17. SECURITY CLASSIFICATION OF REPORT	18. SECURITY CLASSIFICATION OF THIS PAGE	19. SECURITY CLASSIFICATION OF ABSTRACT	20. LIMITATION OF ABSTRACT
Unclassified	Unclassified	Unclassified	